Spatiotemporal variability in carbon exchange fluxes across the Sahel

Tagesson, Torbern; Fensholt, Rasmus; Cappelaere, Bernard; Mougin, Eric; Horion, Stéphanie; Kergoat, Laurent; Nieto, Héctor; Mbow, Cheikh; Ehammer, Andrea; Demarty, Jérôme; Ardö, Jonas

Published in:
Agricultural and Forest Meteorology

DOI:
10.1016/j.agrformet.2016.05.013

2016

Document Version:
Publisher's PDF, also known as Version of record

Agricultural and Forest Meteorology 226–227 (2016) 108–118

Contents lists available at ScienceDirect

Agricultural and Forest Meteorology

journal homepage: www.elsevier.com/locate/agrformet

Spatiotemporal variability in carbon exchange fluxes across the Sahel

Torbern Tagesson[a,*], Rasmus Fensholt[a], Bernard Cappelaere[b], Eric Mougin[c], Stéphanie Horion[a], Laurent Kergoat[c], Héctor Nieto[d], Cheikh Mbow[e], Andrea Ehammer[a], Jérôme Demarty[b], Jonas Ardö[f]

[a] Department of Geosciences and Natural Resource Management, University of Copenhagen, Øster Voldgade 10, DK-1350 Copenhagen, Denmark
[b] Institut de Recherche pour le Développement, HydroSciences Montpellier (CNRS, IRD, UM), BP 64501, 34394 Montpellier Cedex 5, France
[c] Géosciences Environnement Toulouse (GET), UMR 5563 CNRS – UR 234 IRD – UPS, Observatoire Midi-Pyrénées, 14 avenue Edouard Belin, 31400 Toulouse Cedex 4, France
[d] Institute for Sustainable Agriculture (IAS), Spanish National Research Council (CSIC) Campus Alameda del Obispo, Avda. Menendez Pidal s/n 14001 Córdoba, Spain
[e] World Agroforestry Centre, Research Unit SD6, PO Box 30677-00100, Nairobi, Kenya
[f] Department of Physical Geography and Ecosystem Science, Lund University, Sölvegatan 12, SE- 223 62 Lund, Sweden

ARTICLE INFO

Article history:
Received 14 July 2015
Received in revised form 16 May 2016
Accepted 19 May 2016

Keywords:
Carbon dioxide
Climate change
Dryland
Net ecosystem exchange
Photosynthesis
Respiration

ABSTRACT

Semi-arid regions play an increasingly important role as a sink within the global carbon (C) cycle and is the main biome driving inter-annual variability in carbon dioxide (CO_2) uptake by terrestrial ecosystems. This indicates the need for detailed studies of spatiotemporal variability in C cycling for semi-arid ecosystems. We have synthesized data on the land-atmosphere exchange of CO_2 measured with the eddy covariance technique from the six existing sites across the Sahel, one of the largest semi-arid regions in the world. The overall aim of the study is to analyse and quantify the spatiotemporal variability in these fluxes and to analyse to which degree spatiotemporal variation can be explained by hydrological, climatic, edaphic and vegetation variables. All ecosystems were C sinks (average ± total error -162 ± 48 g C m^{-2} y^{-1}), but were smaller when strongly impacted by anthropogenic influences. Spatial and inter-annual variability in the C flux processes indicated a strong resilience to dry conditions, and were correlated with phenological metrics. Gross primary productivity (GPP) was the most important flux process affecting the sink strength, and diurnal variability in GPP was regulated by incoming radiation, whereas seasonal dynamics was closely coupled with phenology, and soil water content. Diurnal variability in ecosystem respiration was regulated by GPP, whereas seasonal variability was strongly coupled to phenology and GPP. A budget for the entire Sahel indicated a strong C sink mitigating the global anthropogenic C emissions. Global circulation models project an increase in temperature, whereas rainfall is projected to decrease for western Sahel and increase for the eastern part, indicating that the C sink will possibly decrease and increase for the western and eastern Sahel, respectively.

1. Introduction

Vegetation growth in semi-arid regions plays an increasingly important role as a sink within the global carbon (C) cycle, and it is the main biome driving inter-annual variability and long-term trends in carbon dioxide (CO_2) uptake by terrestrial ecosystems (Ahlström et al., 2015; Poulter et al., 2014). It has recently been shown that the net ecosystem exchange (NEE) of CO_2 at the peak of the growing season of semiarid savanna ecosystems can potentially reach very high levels (up to -40 μmol CO_2 m^{-2} s^{-1}) (Tagesson et al., 2015a), indicating the importance of improving our understanding of the spatiotemporal variability of C cycling for semi-arid savanna regions across the world.

The African Sahel is a semi-arid savanna region with shrubs and low tree coverage located south of the Sahara desert. The region is characterized by a long dry season and a rainy season of 2–3 months. The livelihood of the Sahelian population is strongly dependent on local ecosystems services providing food, feed, fuel

* Corresponding author.
E-mail addresses: torbern.tagesson@ign.ku.dk (T. Tagesson), rf@ign.ku.dk (R. Fensholt), bernard.cappelaere@um2.fr (B. Cappelaere), eric.mougin@get.obs-mip.fr (E. Mougin), stephanie.horion@ign.ku.dk (S. Horion), laurent.kergoat@get.obs-mip.fr (L. Kergoat), hnieto@ias.csic.es (H. Nieto), C.mbow@cgiar.org (C. Mbow), andrea.ehammer@ign.ku.dk (A. Ehammer), jerome.demarty@univ-montp2.fr (J. Demarty), jonas.ardo@nateko.lu.se (J. Ardö).

http://dx.doi.org/10.1016/j.agrformet.2016.05.013
0168-1923/

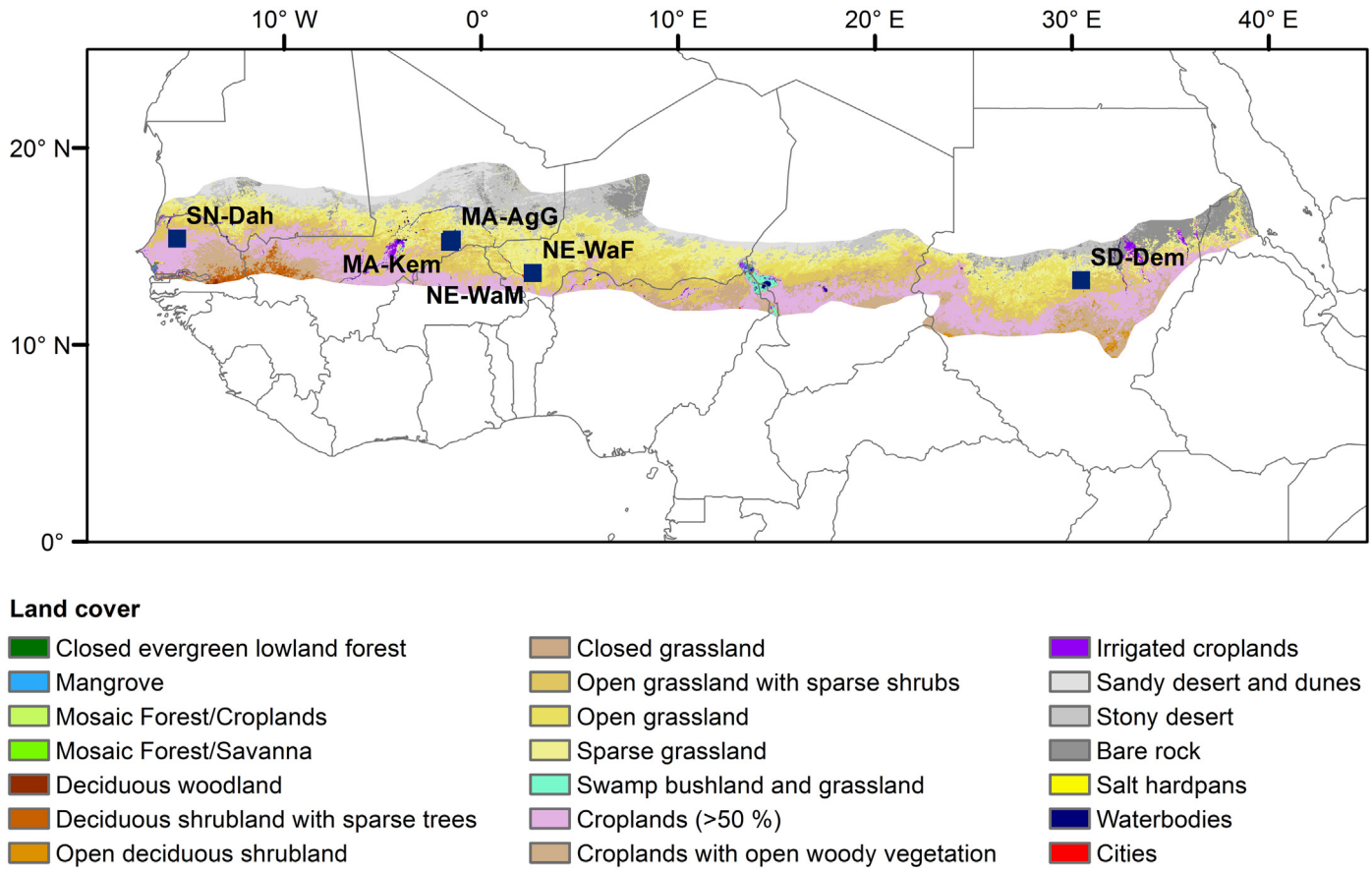

Fig. 1. Location of the different sites in the Sahel. Land cover for the Sahel (based on multi-sensor satellite observations (Mayaux et al., 2003)) and location of the different sites included in the study. The sites are Demokeya (SD-Dem), Agoufou (ML-AgG), Kelma (ML-Kem), Dahra (SN-Dah), Wankama Fallow (NE-WaF), and Wankama Millet (NE-WaM). The delineation of the Sahel is based on isohyets 150 and 700 mm.

and fibre, but Sahelian ecosystems are currently under great pressure from rapidly increasing population, changes in land-use and climatic forcing (Abdi et al., 2014; Sarr, 2012). In the future, it is projected that the Sahel will have shorter rainy seasons, increased temperature and increased or decreased rainfall, depending on location within the Sahel (Roehrig et al., 2013; Sarr, 2012). This will affect the ecosystem productivity with consequences for Sahelian livelihood strategies (OECD, 2009; Sarr, 2012). An improved understanding of resilience and responses of these ecosystems to climatic and environmental changes are therefore essential to better understand, quantify, and predict the effects of current and future climate change.

The NEE is the balance between CO_2 assimilated through gross primary productivity (GPP) by the vegetation and the C decomposed and released as ecosystem respiration (R_{eco}). There is great spatiotemporal variability in climatic, hydrological, edaphic, and vegetation factors across the Sahel, and the NEE and the C exchange processes (GPP and R_{eco}) are known to vary considerably both spatially and temporally for semi-arid savanna areas (e.g. Merbold et al., 2009; Moncrieff et al., 1997). Merbold et al. (2009) explained the variability in CO_2 exchange across the African biomes with annual sums of rainfall and Brümmer et al. (2008) have shown the importance of water availability and rainfall distribution for inter-annual variation in C budgets for a Soudanian savanna ecosystem. Moncrieff et al. (1997) showed that phenology was the main factor determining CO_2 flux variability, both in space and in time, which in turn was mainly determined by the timing of the start of the rainy season. Rockström and de Rouw (1997) on the other hand showed that short periods of intra-seasonal drought have a larger effect on spatiotemporal variability in grain yield than the annual sums of rainfall for a millet farm in the Sahel. Instead, it was nutrient availability increasing the capacity to compensate for damage caused by water shortage determining the size of grain yield (Rockström and de Rouw, 1997). The biomass accumulation and C exchange processes can also vary considerably depending on species composition, thus affecting both the spatial and inter-annual variation (Boulain et al., 2009; Mbow et al., 2013). Tagesson et al. (2016) explained findings of high CO_2 exchange fluxes at the peak of the rainy season for a grazed semi-arid savanna site in Senegal with alleviated water stress conditions, a low C3/C4 ratio and a grazing pressure resulting in compensatory growth and fertilization effects. Hence, there is a range of explanatory variables describing variability in the land-atmosphere C exchange processes for semi-arid savanna ecosystems, which indicates the importance of analysing and quantifying these relationships at different temporal and spatial scales.

A method that has received much attention during recent decades is the eddy covariance (EC) technique, which has become an important tool for measuring the CO_2 exchange between land and atmosphere. The EC method provides high resolution long term temporal data, making it suitable for assessing the diurnal, seasonal and inter-annual variation of net C exchange at the ecosystem level. Compared to boreal and temperate ecosystems, semi-arid savanna regions of Africa are underrepresented in the global EC flux networks (Ardö et al., 2008; Schwalm et al., 2010). However, a limited number of sites with conducted EC measurements does exist in the Sahel, and data from these sites are now available from the Fluxnet database, a global network of micrometeorological measurement

sites (Baldocchi et al., 2001). In order to study spatial and temporal variability for the semi-arid ecosystems of the Sahel we have synthesized the NEE and the C exchange processes (GPP and R_{eco}) as represented by existing available EC data. Research questions motivating this study are: To which degree can driving factors influencing the C exchange processes be used to determine the fluxes at diurnal, seasonal, and inter-annual scale? Can the Sahel be considered as a homogenous or heterogeneous region regarding the C sink/source strength, and to which degree can driving factors be used to determine this spatial variability? Finally, can these relationships be used for improving our understanding of the role of the entire Sahel on the global C balance?

2. Material and methods

2.1. Experimental sites

The Sahel is an ecoclimatic and biogeographic transition zone between the Sahara desert to the north and the Soudanian Savanna to the south stretching from the Atlantic Ocean to the Red Sea (Fig. 1). The extent of Sahel is defined as the region receiving between 150 and 700 mm rainfall per year (Prince et al., 1995). We have used EC data of NEE from six semi-arid savanna sites across the Sahel (Table 1; Fig. 1). The sites represent a variety of natural and cultivated semi-arid ecosystems of the Sahel, from Senegal in the west to Sudan in the east, and from a dry fallow bush region to a seasonally inundated acacia forest. For description of the different sites, we refer to Table 1 and references therein.

2.2. Eddy covariance and ancillary data

The sites are registered at the Fluxnet database, and EC and ancillary data were collected from the principal investigators. Data cover the years between 2005 and 2013, with available data from between one and four years from each site (Table 1). The EC systems consisted of 3-axis sonic anemometers, and open-path CO_2/H_2O infrared gas analysers. The sonic anemometer and gas analyser data were sampled at 20 Hz rate, and the fluxes were calculated for 30 min periods. We extracted the level 2 original NEE data, without any gap filling and partitioning of NEE to GPP and R_{eco} applied to the datasets. The fluxes were filtered according to the Fluxnet quality control flags, (only good data were used; quality control flag = 0). Outliers were additionally filtered according Papale et al. (2006). Many of the sites have big data gaps, and a lot of filtered data (Table 1). However, Falge et al. (2001) found that on average 35% of EC data are generally missing, whereas Papale et al. (2006) estimated that 20–60% of the data were rejected by the different quality filters applied. The EC systems were running throughout most of the rainy seasons, capturing the part of the year with high NEE variability, and the long gaps mainly occurred during the dry seasons, characterised by stable fluxes and limited vegetation activity. All sites are located in remote areas with limited research activities during the dry seasons, including also a lower maintenance frequency of the EC systems causing longer gaps in cases of instrumental malfunctioning. Additionally, in case there was need for any sensor repair this was done during the dry seasons.

We collected hydrological, meteorological, edaphic, and vegetation data from the individual sites; air and soil temperature (T_{air}, and T_{soil} (0.1 m depth), respectively; °C), rainfall (P; mm), relative air humidity (Rh; %), soil moisture at 0.1 m depth (SWC; % volumetric water content), incoming global radiation (R_g; W m^{-2}), incoming photosynthetically active radiation (PAR; μmol m^{-2} s^{-1}), vapour pressure deficit (VPD; hPa), herbaceous peak dry weight biomass (g DW m^{-2}), C3/C4 species ratio, and soil nitrogen and C content (%) (Table 2).

For investigating the relationship between the C exchange fluxes and vegetation phenology, we collected remotely sensed composite products from the Moderate Resolution Imaging Spectroradiometer (MODIS)/Terra L3 & L4 from the NASA Earth Observing System (EOS) data gateway. The obtained products were the normalized difference vegetation index (NDVI) (MOD13Q1) at 250 m spatial resolution, and leaf area index (LAI) and fraction of photosynthetically active radiation absorbed by the green vegetation (FPAR) (MOD15A2) at 1 km spatial resolution. The time series of the MODIS products were filtered according to the MODIS quality control data (MODLAND QC) and gap-filled using linear interpolation. Annual maximum values ($_{max}$) of the remotely sensed products were extracted. Integrals of vegetation indices are often used as metrics for vegetation productivity within the earth observation community (e.g. Bai et al., 2008; Fensholt et al., 2015; Tucker et al., 1983) and annual sums ($_{sum}$) were therefore calculated. Additional metrics from NDVI were growing season integral ($_{int}$), start, end and length of the growing season, and these were computed using a Savitsky–Golay filtering technique available in the TIMESAT software (Jönsson and Eklundh, 2004). The parameters applied in the TIMESAT analysis were: NDVI data range = 0.1-1.0, seasonal parameter = 0.5, Number of envelope iterations = 3, adaptation strength = 1, Savitzky–Golay window size = 3, and amplitude season start and end = 0.2 (Jönsson and Eklundh, 2004). For a further description of the TIMESAT software and the parameters, see Jönsson and Eklundh (2004).

2.3. Data analysis

2.3.1. Short term controls on half-hourly CO_2 exchange fluxes

We used a 20 W m^{-2} R_g threshold to separate the half-hourly NEE into daytime and night-time data. To investigate the drivers of short term variability in CO_2 exchange across the Sahel, daytime and night-time half-hourly NEE were analysed for linear and exponential relationships to ancillary data (T_{air}, T_{soil}, Rh, SWC, R_g, PAR, and VPD) using ordinary least square single variable regressions during 7-day moving windows. Only measured data without any gap-filling were included in this analysis and the 7-day moving windows were used in order to avoid seasonal auto-correlation. The effect of incoming PAR on daytime-NEE was additionally estimated for each 7-day moving window using non-linear Mitscherlich light-response functions following the equation used by Aubinet et al. (2001), Lindroth et al. (2008) and Reichstein et al. (2012):

$$NEE = -(F_{csat} + R_d) \times \left(1 - \exp\left(\frac{-\alpha \times PAR}{F_{csat} + R_d}\right)\right) + R_d \quad (1)$$

where F_{csat} is the optimized NEE at light saturation (μmol CO_2 m^{-2} s^{-1}), R_d is dark respiration (μmol CO_2 m^{-2} s^{-1}) and α is the quantum efficiency (μmol CO_2 μmol PAR^{-1}) or the initial slope of the light response curve. Ecosystem respiration is generally considered to follow an exponential relationship against temperature. An equation originally derived for soil respiration by Lloyd and Taylor (1994) is commonly used for testing the relationship between ecosystem respiration and temperature:

$$R_{eco} = R_{10} \times \exp\left(\frac{1}{56.02} - \frac{1}{T + 273015 - 227.13}\right) \quad (2)$$

where R_{10} is the respiration rate (μmol CO_2 m^{-2} s^{-1}) at 10 °C, and T is the temperature (°C) (Falge et al., 2001; Lloyd and Taylor, 1994; Reichstein et al., 2005, 2012). We fitted equation 2 with night-time NEE against air temperature, and soil temperature for each 7-day moving window.

2.3.2. Partitioning and gap-filling half-hourly CO_2 exchange fluxes

From the Fluxnet data base, partitioned data is available using temperature response curves following a standardized method by

Table 1
Site description including location, ecosystem type, dominant species, soil classification, measurement period and sensor set up for the eddy covariance system of the different sites. Height is measurement height of the sensors.

Site	Coordinates	Ecosystem	Dominant species	Soil classification	Years	Gas analyser	Sonic anemometer	Data availability	Height (m)
Demokeya[a] (SD-Dem, Sudan)	13.28°N, 30.48°E	Sparse acacia savanna (7% tree cover)	Trees: *Acacia spp.*, Herbs: *Aristida pallida, Eragrostis tremula, Cenchrus biflorus*	Cambic Arenosol	2007–2009	LiCor 7500	GILL R3 (GILL Instruments)	0.43	9
Agoufou[b] (ML-AgG, Mali)	15.34°N, 1.48°W	Open woody savanna (4% tree cover)	Trees: *Acacia spp., Balanites aegyptiaca, Combretum glutinosum* Herbs: *Zornia glochidiata, Cenchrus biflorus, Aristida mutabilis, Tragus berteronianus*	Sandy ferruginous Arenosol	2007	LiCor 7500	Csat-3 (Campbell Scientific)	0.40	4.2
Kelma[b] (MA-Kem, Mali)	15.22°N, 1.57°W	Seasonally flooded open woodland (90% tree cover)	Trees: *Acacia seyal, Acacia nilotica, Balanites aegyptiaca* Herbs: *Sporobolus hevolvus, Echinochloa colona, Aeschinomene sensitive*	Clay soil depression	2007	LiCor 7500	Csat-3 (Campbell Scientific)	0.45	12
Dahra[c] (SN-Dah, Senegal)	15.40°N, 15.43°W	Grassland/shrubland Savanna (3% tree cover)	Trees: *Acacia spp., Balanites aegyptiaca* Herbs: *Zornia latifolia, Aristida adscensionis, Cenchrus biflorus*	Sandy luvic Arenosol	2010–2013	LiCor 7500	GILL R3 (GILL Instruments)	0.26	9
Wankama Fallow[d] (NE-WaF, Niger)	13.65°N, 2.63°E	Fallow bush	Trees: *Guiera senegalensis* Herbs: *Cenchrus biflorus, Zornia glochidiata, Mitracarpus scaber*	Sandy ferruginous Arenosol	2005–2006	LiCor 7500	Csat-3 (Campbell Scientific)	0.47	5
Wankama Millet[e] (NE-WaM, Niger)	13.64°N, 2.63°E	Millet crop	Crop: *Pennisetum glaucum* Residual, cut-back trees: *Guiera senegalensis*	Sandy ferruginous Arenosol	2005–2006	LiCor 7500	Csat-3 (Campbell Scientific)	0.42	5.1

[a] Sjöström et al. (2009).
[b] Mougin et al. (2009).
[c] Tagesson et al. (2015b).
[d] Ramier et al. (2009).
[e] Boulain et al. (2009).

Table 2
Annual values of hydrological, meteorological, edaphic and vegetation variables for the different sites. The biomass is the dry weight (DW) herbaceous biomass measured at the peak of the growing season; P is rainfall; N and C cont. are soil nitrogen and carbon contents at 0–20 cm depth; T_{air} and T_{soil} are air temperature at 2 m height and soil temperature at 0.1 m depth, respectively; SWC is soil water content (% volumetric water content) measured at 0.1 m soil depth; Rh is relative humidity, VPD is vapour pressure deficit, R_g is incoming global radiation and PAR is photosynthetically active radiation. The sites are Demokeya (SD-Dem), Agoufou (ML-AgG), Kelma (ML-Kem), Dahra (SN-Dah), Wankama Fallow (NE-WaF), and Wankama Millet (NE-WaM). – means no data.

Site	Year	Biomass(g DW m^{-2})	C3/C4 ratio	P(mm)	N cont. (%)	C cont. (%)	T_{air} (°C)	T_{soil} (°C)	SWC (%)	Rh(%)	VPD (hPa)	Rg(W m^{-2})	PAR(μmol m^{-2} s^{-1})
SD-Dem	2007	92	0.30	356	0.027	0.09	27.0	33.0	4.2	35.2	25	264	521
SD-Dem	2008	99	0.30	293	0.027[a]	0.09[a]	27.1	32.7	4.2	36.5	25	257	511
SD-Dem	2009	59	0.30	238	0.027[a]	0.09[a]	27.9	33.7	3.6	31.1	28	253	480
ML-AgG	2007	162	0.25	349	0.033[b]	0.20[b]	29.2	30.0[d]	1.8[d]	31.2	31	262	499
ML-Kem	2007	–	0.90	349	0.069[b]	0.45[b]	28.4	31.5	–	33.6	28	254	488[e]
SN-Dah	2010	471	0.19	650	0.037[c]	0.38[c]	28.6	33.9	3.9	41.8	35	237	449
SN-Dah	2011	223	0.19	486	0.040	0.32	27.9	33.3	3.9	39.9	37	244	473
SN-Dah	2012	206	0.19	606	0.034	0.43	28.1	34.0	4.7	41.6	37	233	471
SN-Dah	2013	265	0.19	355	0.037[c]	0.38[c]	28.5	33.8	4.4	41.5	40	239	498
NE-WaF	2005	71	0.80	495	–	–	29.7	33.1	1.3	34.7	44	242	468[e]
NE-WaF	2006	132	0.80	572	–	–	29.5	33.2	1.7	36.4	42	244	472[e]
NE-WaM	2005	201	0.10	495	–	–	29.0	31.8	2.3	33.3	43	247	479[e]
NE-WaM	2006	130	0.10	572	–	–	28.5	31.0	2.8	35.8	28	245	475[e]

[a] Measured in 2007.
[b] Measured in 2006.
[c] Average of 2011–2012.
[d] Measured at 0.05 m depth.
[e] Modelled from R_g.

Reichstein et al. (2005). No short term relationship between night-time NEE and temperature during 7-day moving windows at these Sahelian sites were observed (for results see subsection 3.1). The daytime NEE measured at all sites were thereby partitioned into GPP and R_{eco} following the method by Falge et al. (2001), using the Mitscherlich light-response function (Eq. (1)). Vapour pressure deficit limits on GPP was accounted for by replacing the fixed F_{csat} parameter in Eq. (1) with an exponential decreasing function:

$$F_{csat} = \begin{cases} F_{csat}\exp^{-k\,VPD-VPD_0} & VPD > VPD_0 \\ F_{csat} & VPD < VPD_0 \end{cases} \qquad VPD_0 = 10hPa \qquad (3)$$

following the method by Lasslop et al. (2010). Eq. (1) in combination with Eq. (3) was parameterized for daytime NEE using the 7-day moving windows throughout the measurement periods. By subtracting R_d the functions were forced through 0, and GPP was thereby estimated:

$$GPP = -(F_{csat} + R_d) \times \left(1 - \exp\left(\frac{-\alpha \times PAR}{F_{csat}+R_d}\right)\right) \qquad (4)$$

Ecosystem respiration was subsequently calculated by subtracting modelled GPP from measured NEE.

Gaps shorter than three days in the time series of NEE, GPP and R_{eco} were consequently gap-filled, following Falge et al. (2001): (1) gaps shorter than 2 h were filled using linear interpolation; (2) daytime gaps longer than 2 h were filled using Eqs. (1) and (3) for NEE, and Eqs. (3) and (4) for GPP fitted to half-hourly NEE values from 7-day moving windows; (3) night-time GPP was set to 0, and gaps in night-time NEE were set to average NEE measured during that night; (4) mean diurnal variation calculated for the 7-days moving windows were used for filling any remaining gaps shorter than three days; (5) finally, gap-filled GPP was subtracted from gap-filled NEE to estimate gap-filled R_{eco}. This first calculation step gives negative GPP values; in order to clarify results from the correlation analysis we converted GPP to positive values. A source of error in the gap-filling is that data during low turbulent conditions are filtered out, and hence underrepresented in the application of the gap filling. However, there was no correlation between NEE and friction velocity within 7-day moving windows for any of the sites indicating no strong influence of turbulence on the measurements.

2.3.3. Seasonal, spatial and inter-annual dynamics of the C exchange fluxes

The seasonal dynamics in NEE, R_{eco} and GPP interact in complicated non-linear ways with environmental variability, and ordinary regression models that are supposed to apply over the entire data space do not perform well. Therefore, daily sums of NEE, R_{eco} and GPP were calculated from the gap-filled time-series and relationships to the ancillary data were analysed using regression tree analysis. This is a robust non-parametric statistical method to study complex, nonlinear relationships between a response variable and several explanatory variables (De'ath and Fabricius, 2000). The ancillary data included in the regression tree analysis were daily values of: NDVI, T_{air}, T_{soil}, Rh, SWC, PAR, and VPD. The data were split into homogeneous subgroups categorized by values of the

Table 3
Statistics for the regression tree analysis studying relationships between seasonal dynamics in the land-atmosphere C exchange processes and the explanatory variables. NEE is net ecosystem exchange, GPP is gross primary productivity, R_{eco} is ecosystem respiration, R^2 is the coefficient of determination for the regression tree, NDVI is the normalized difference vegetation index, PAR is photosynthetically active radiation (μmol m^{-2} s^{-1}), VPD is vapour pressure deficit (hPa), SWC is soil water content at 0.1 m soil depth (% volumetric water content), T_{soil} and T_{air} is soil temperature at 0.1 m soil depth and air temperature at 2 m height (°C), respectively. The sites are Demokeya (SD-Dem), Agoufou (ML-AgG), Kelma (ML-Kem), Dahra (SN-Dah), Wankama Fallow (NE-WaF), and Wankama Millet (NE-WaM). The pruning level is the number of splits of the regression tree.

Explanatory variables:	1	2	3	4	5	6	Pruning level	R^2
NEE (g C m^{-2} d^{-1})								
SD-Dem	NDVI	T_{soil}	PAR	SWC	VPD	T_{air}	20	0.81
ML-AgG	NDVI	SWC[a]	PAR				6	0.85
ML-Kem	NDVI	PAR					6	0.78
SN-Dah	NDVI	PAR	VPD	SWC	T_{soil}	T_{air}	17	0.77
NE-WaF	NDVI	SWC	T_{soil}	PAR	T_{air}	VPD	16	0.79
NE-WaM	SWC	NDVI					2	0.17
GPP (g C m^{-2} d^{-1})								
SD-Dem	NDVI	VPD	SWC	PAR	T_{air}		88	0.98
ML-AgG	NDVI	SWC[a]	PAR	T_{air}			10	0.98
ML-Kem	NDVI	PAR	VPD	T_{air}			26	0.97
SN-Dah	NDVI	SWC	PAR	VPD	T_{air}		54	0.96
NE-WaF	NDVI	SWC	VPD	PAR			18	0.94
NE-WaM	NDVI	T_{air}	SWC	VPD	PAR		19	0.72
R_{eco} (g C m^{-2} d^{-1})								
SD-Dem	GPP	SWC	VPD	T_{soil}	NDVI		24	0.83
ML-AgG	NDVI	SWC[a]	GPP	VPD	T_{soil}		14	0.96
ML-Kem	NDVI	VPD	GPP	T_{soil}			26	0. 74
SN-Dah	GPP	NDVI	SWC	VPD	T_{soil}		27	0.91
NE-WaF	NDVI	SWC	T_{soil}	VPD	GPP		16	0.89
NE-WaM	NDVI	GPP	T_{soil}				3	0.27

[a] Measured at 0.05 m depth.

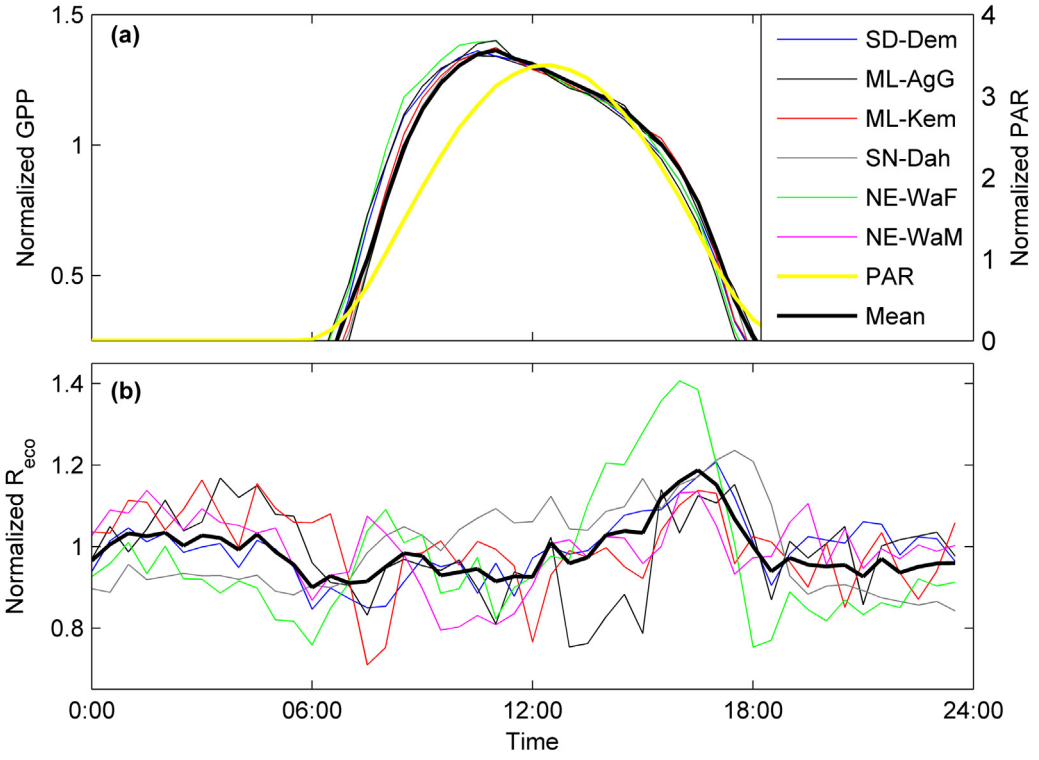

Fig. 2. Diurnal patterns in the land atmosphere exchange processes. Median diurnal patterns in (a) gross primary productivity (GPP), photosynthetically active radiation (PAR), and (b) ecosystem respiration (R_{eco}) for Demokeya (SD-Dem), Agoufou (ML-AgG), Kelma (ML-Kem), Dahra (SN-Dah), Wankama Fallow (NE-WaF), and Wankama Millet (NE-WaM). The normalization was done by dividing each half-hourly value by the mean daily value. We only used data from days with more than 70% data coverage.

dependent and the independent variables. The splitting creates a large tree, which was pruned to an appropriate size using cross validation. The data were separated into ten subgroups of about equal size, and at least five days were required in each subgroup. Ten trees were created with nine of the subgroups, one was left out, and the ten trees were evaluated against the left-out subgroup. For each of the ten trees, the error was summed and the smallest tree with the lowest error was selected. We repeated the procedure 100 times, and the tree size that was most common was used in the final analysis. For a detailed description of the advantages with regression tree analysis, see De'ath and Fabricius (2000).

Regression trees were also used for filling remaining gaps longer than three days in the CO_2 fluxes. 100 tree sizes were chosen based on 100 runs of cross validation, and these trees were used for estimating the CO_2 fluxes (De'ath and Fabricius, 2000). The 100 CO_2 flux subsets were averaged and used for filling the gaps in daily sums of NEE, GPP and R_{eco}. A source of error in the gap filling of daily sums of the CO_2 fluxes is the long data gaps during the dry seasons. However, because of the limited vegetation activity during this period of the year, flux variability is low and fluxes are very stable. All sites had sampled data from the dry seasons, which were used within the regression trees for filling these gaps.

We calculated total annual C budgets by summing all NEE, GPP and R_{eco} fluxes for each year. To study the drivers of spatial and inter-annual variability in CO_2 exchange across the six sites in Sahel, annual sums of NEE, GPP, and R_{eco} were correlated with ancillary data using ordinary Pearson linear correlation. GPP and R_{eco} are derived from NEE and these variables are thereby spuriously correlated (Brett, 2004). In order to avoid the spurious correlation when analysing the relationship between NEE, GPP, and R_{eco} we used a bootstrap simulation methodology where the NEE, GPP, and R_{eco} datasets were copied and randomly sorted 1000 times (Brett, 2004). The 1000 randomly sorted datasets of GPP and R_{eco} were subtracted from the 1000 random datasets of NEE resulting in 1000 random datasets of R_{eco} and GPP, respectively. The spurious correlation was estimated by correlating these 1000 random datasets, and accounted for in the correlation between the original NEE, GPP, and R_{eco} datasets following the method by Brett (2004) and Lund et al. (2010).

There are uncertainties built in to the EC method which affect the long term CO_2 budgets and it is therefore essential to quantify errors in the budgets. Given that data were collected at Fluxnet, it is not possible to estimate the random and systematic error of each individual turbulent flux measurement. However, it is commonly accepted that uncertainty for individual turbulent flux measurements are 10–20% (Moncrieff et al., 1996), and we thereby applied an uncertainty factor of 15% to each individual flux measured value (E_{meas}). Uncertainties related to gap filling using light response functions (E_{gap_light}) can be estimated by using different subsets when parameterising the gap-filling model (Papale, 2012). We used a bootstrap simulation methodology, where the datasets were copied 100 times for each 7-day moving window (Richter et al., 2012). The runs generated 100 sets of parameters for Eqs. (1), (3) and (4) and E_{gap_light} was estimated from the uncertainty in 100 budgets calculated using these 100 sets of parameters. The errors associated with the gap-filling using the average night-time data and the mean diurnal variation was estimated from the standard deviation (E_{gap_mean}). The errors associated with filling gaps longer than 3 days using regression tree analysis (E_{gap_tree}) were estimated from the uncertainty in 100 CO_2 flux estimates from the regression trees. All gap filling errors were considered as systematic given that the gap-filling methods differed for different parts of the day and that the longer gaps were not randomly distributed throughout the year (Moncrieff et al., 1996).

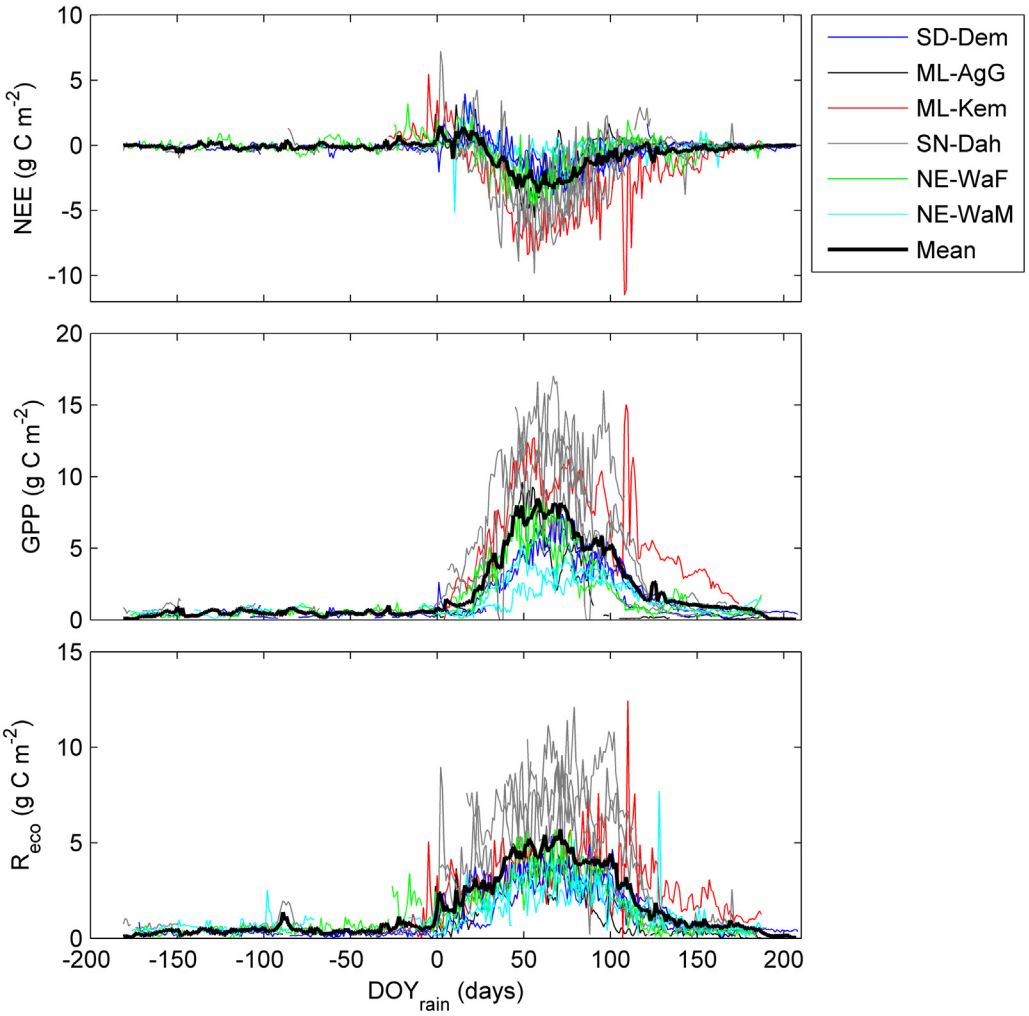

Fig. 3. Seasonal patterns in the land atmosphere exchange processes. Seasonal patterns in net ecosystem exchange (NEE), gross primary productivity (GPP) and ecosystem respiration (R_{eco}). DOY_{rain} is set to equal 0 the day of year (DOY) when the rainy season starts. The rainy season is defined to start the first DOY with rainfall (occasionally there were minor rainfall events before the actual start of the rainy season and these are not included). The sites are Demokeya (SD-Dem), Agoufou (ML-AgG), Kelma (ML-Kem), Dahra (SN-Dah), Wankama Fallow (NE-WaF), and Wankama Millet (NE-WaM).

3. Results

3.1. Diurnal variability in CO_2 exchange fluxes

Half-hourly GPP peaked in the morning at 11:00-11:30, slightly before the peak of incoming radiation (Fig. 2a). Average R_{eco} was at minimum in the morning at 11:00 and peaked late in the afternoon at 17:00 (Fig. 2b). All sites except Dahra followed the average diurnal R_{eco} curve, whereas Dahra had lowest values during night-time. None of the sites had any strong relationships between night-time half-hourly NEE and any of the explanatory variables for the 7-day periods throughout neither the rainy nor the dry season. The main factor determining the daytime half-hourly NEE was PAR, as there were strong relationships following the Mitscherlich function (Eq. (1)) for all sites and throughout most of the seasonal cycles. There were, however, days during the dry season and during the start and end of the rainy season without a relationship. During the dry season, limited productivity was observed. In the beginning of the rainy season, there were large bursts in R_{eco} (Fig. 3) which conceals the minor productivity at this state of the phenological cycle.

3.2. Seasonal dynamics in CO_2 exchanges

The overall seasonal dynamics were similar across all sites, but differences in the amplitude were observed (Fig. 3). The ecosystems were more or less C neutral during the dry season, and NEE were low (average NEE 1 December to 1 June all sites: $-0.11 \pm 0.18\,g\,C\,m^{-2}\,d^{-1}$). There was no herbaceous vegetation and the minor dry season GPP (average GPP 1 December to 1 June all sites: $0.52 \pm 0.15\,g\,C\,m^{-2}\,d^{-1}$) was from some few evergreen trees. Ecosystem respiration was also low (average R_{eco} 1 December to 1 June all sites: $0.44 \pm 0.16\,g\,C\,m^{-2}\,d^{-1}$), due to the low SWC (average SWC 1 December to 1 June all sites: 1.9 ± 0.13%Vol) decreasing microbial activity. The effect of the start of the rainy season on the CO_2 exchange processes was clear (Fig. 3); soil decomposers were activated due to the increased SWC and there was a strong increase in R_{eco}. The R_{eco} exceeded the GPP, and the ecosystem acted as a C source. However, herbaceous vegetation also responded to the increased SWC, and subsequently started to grow. Gross primary productivity increased with biomass turning the ecosystem into a C sink when GPP exceeded the R_{eco}. For the peak of the rainy season, daily average peak (highest annual value of a 15 day running mean) NEE rates for all sites were $-3.69\,g\,C\,m^{-2}\,d^{-1}$, but with a large range of between $-0.90\,g\,C\,m^{-2}\,d^{-1}$ (Wankama Millet 2006)

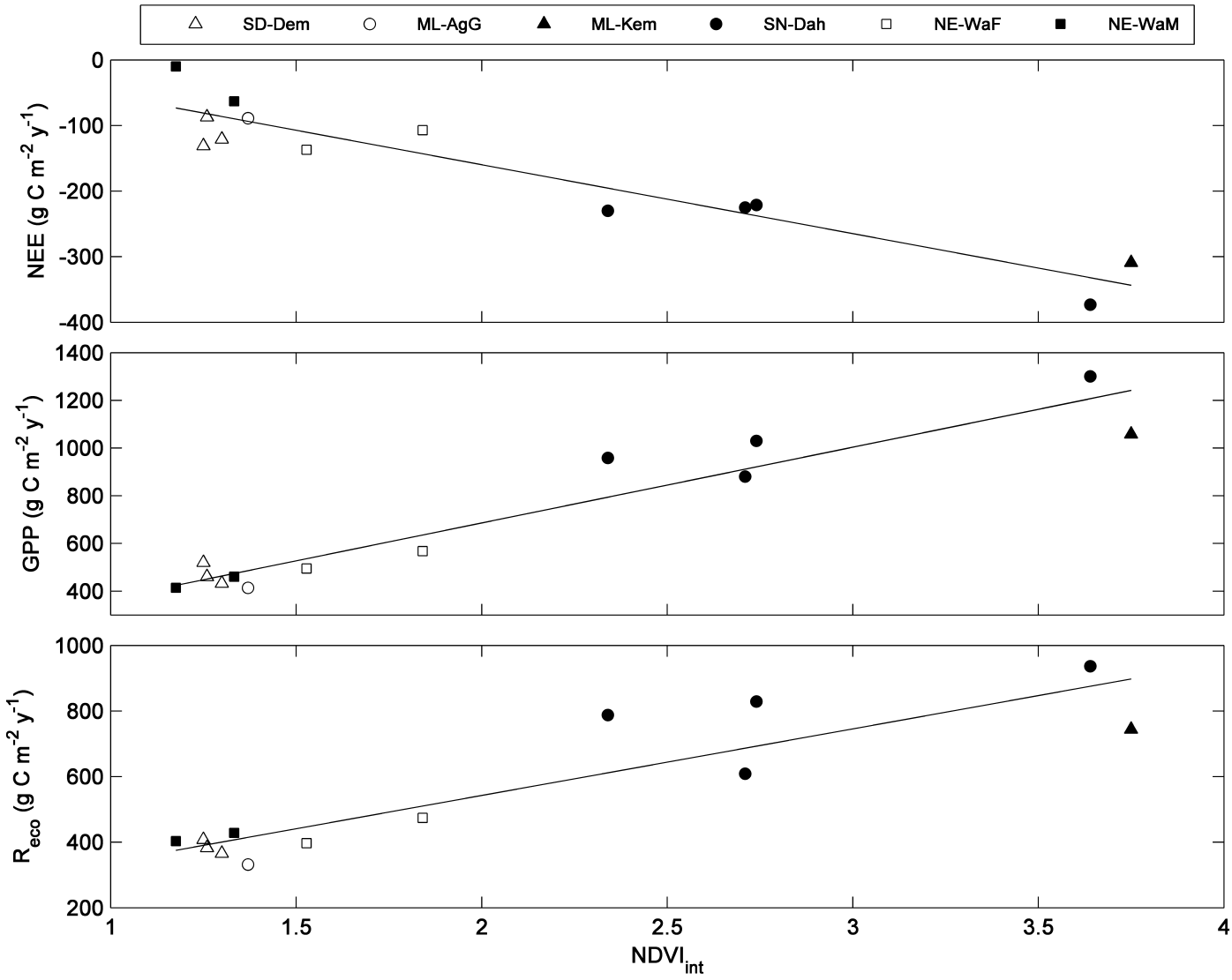

Fig. 4. Scatter plot of among-site and inter-annual budgets of the land atmosphere exchange processes against the seasonal integral of the normalized difference vegetation index ($NDVI_{int}$). $NDVI_{int}$ was the explanatory variables of strongest correlation. (a) Net ecosystem exchange (NEE); (b) gross primary productivity (GPP), and (c) ecosystem respiration (R_{eco}). The sites are Demokeya (SD-Dem), Agoufou (ML-AgG), Kelma (ML-Kem), Dahra (SN-Dah), Wankama Fallow (NE-WaF), and Wankama Millet (NE-WaM). The black lines are the ordinary least-square linear regression lines.

and $-7.02\,g\,C\,m^{-2}\,d^{-1}$ (Kelma 2007). Average peak GPP and R_{eco} rates were $8.34\,g\,C\,m^{-2}\,d^{-1}$ and $5.04\,g\,C\,m^{-2}\,d^{-1}$ respectively. The range was between $3.39\,g\,C\,m^{-2}\,d^{-1}$ and $14.41\,g\,C\,m^{-2}\,d^{-1}$ for GPP and $2.84\,g\,C\,m^{-2}\,d^{-1}$ and $9.59\,g\,C\,m^{-2}\,d^{-1}$ for R_{eco}. Dahra 2010 had the highest absolute values for both GPP and R_{eco}, and Wankama Millet 2006 the lowest for GPP and Demokeya 2007 the lowest for R_{eco}. The ecosystems continued to be C sinks until the end of the rainy season (Fig. 3).

All variables included in the regression tree analysis are repeated observations characterized by temporal auto-correlation and are thereby not statistically independent. It is therefore not possible to estimate the exact contribution of each of the explanatory variables controlling the CO_2 fluxes, but the regression tree analysis does indicate which explanatory variables that are closest coupled to the CO_2 fluxes. The regression trees explained the variability in CO_2 fluxes well for all sites except for NEE at Wankama Millet (Table 3). The main explanatory variables (in the order mentioned) coupled to seasonal dynamics in NEE were: NDVI, SWC, PAR, T_{soil}, VPD, and T_{air}. Variables coupled to seasonal dynamics in GPP were: NDVI, SWC, PAR, VPD, and T_{air}. For the analysis of seasonal dynamics in R_{eco} the main explanatory variables were: NDVI, GPP, SWC, VPD, and T_{soil}.

3.3. Spatial and inter-annual dynamics in CO_2 fluxes

Large spatial and inter-annual variability in the CO_2 fluxes were found across the six sites in the Sahel (Table 4). The average yearly NEE was $-162 \pm 47\,g\,C\,m^{-2}\,y^{-1}$ (annual budget ± total error). On average, all sites acted as C sinks ranging between $-10 \pm 29\,g\,C\,m^{-2}\,y^{-1}$ to $-373 \pm 80 C\,m^{-2}\,y^{-1}$; with the smallest and largest sink strength at Wankama Millet 2006 and Dahra 2010, respectively. Also large inter-annual and spatial variability in GPP and R_{eco} was observed; GPP ranged between 414 ± 54 to $1301 \pm 124\,g\,C\,m^{-2}\,y^{-1}$ (average: $692 \pm 88\,g\,C\,m^{-2}\,y^{-1}$) and R_{eco} ranged between 332 ± 31 and $937 \pm 94\,g\,C\,m^{-2}\,y^{-1}$ (average: $546 \pm 60\,g\,C\,m^{-2}\,y^{-1}$). Again Dahra was characterised by the highest absolute values of annual GPP and R_{eco}, whereas Agoufou showed the lowest.

There were strong negative correlations between annual NEE and GPP and R_{eco} budgets, also after taking the spurious correlation

stemming from the partitioning procedure into account, indicating that sites with high GPP and R_{eco} were strong C sinks (Table 5). It was also shown that sites with high Rh, biomass, and soil C content, and high values of phenology metrics (LAI_{max}, $FPAR_{max}$, $NDVI_{max}$, $NDVI_{sum}$, and $NDVI_{int}$) were strong C sinks. Annual GPP was correlated with Rh, R_g, biomass, soil C contents, and all phenology metrics. Annual R_{eco} was correlated with P, Rh, R_g, biomass, soil C contents, and all phenology metrics. $NDVI_{int}$ was found to be the metric with the strongest correlations to NEE, GPP and R_{eco} (Table 5, Fig. 4).

4. Discussion

One of the main characteristics of the Sahelian environment, and for semi-arid areas in general, is the dry season suppressing GPP and R_{eco} for a long period of the year (>200 days) (Fig. 3). Even though there was among-site variations in meteorology, nutrient availability, species composition, and ecosystem structure (Table 1), all sites are characterized by long dry seasons. The among-site variation in GPP was higher than the among-site variation in R_{eco} (range: 887 and 605 g C m^{-2} y^{-1} and coefficient of variation: 0.45 and 0.38, respectively), indicating that R_{eco} was more suppressed than was GPP by these dry conditions. Consequently, GPP of the Sahel is more variable than R_{eco}, and factors regulating GPP are fundamental for the inter-annual variability in the C balance of the Sahel.

Limited variability in night-time NEE was observed, and there was no correlation between night-time NEE and temperature. The diurnal pattern (Fig. 2) is noticeable and indicates that photosynthesis could be the main driver of short-term variability in R_{eco}, but with a time-lag (Tang et al., 2005). Ecosystem respiration would then instead be constrained by substrate availability, and the time-lag is due to the fact that photosynthetic products (mainly carbohydrates) needs some time for the translocation downwards from the leaves to the roots (Tang et al., 2005). The R_{eco} thereby peaks when the carbohydrate reaches the roots, a couple of hours after the daytime GPP peak (Fig. 2). The only site which deviated from this pattern was Dahra, being characterised by high GPP values, possibly giving high substrate availability for heterotrophic respiration resulting in high R_{eco} throughout the day (Fig. 2). Seasonal dynamics in R_{eco} was also strongly affected by GPP for many of the sites (Table 3), indicating a strong impact of ecosystem productivity on R_{eco} (e.g. Flanagan and Johnson, 2005; Janssens et al., 2001).

Surprisingly, no correlation between length of growing season and annual budgets of GPP was found (Table 5). The lack of relationship could possibly be explained by the dominance of short-lived annual herbaceous species of the Sahel that are specialized to grow quickly at the beginning of the rainy season (Elberse and Breman, 1989, 1990; Mbow et al., 2013), and thereby not very much affected by the length of the rainy season. The bulk of herbaceous production also occurred during the first few weeks in the AMMA-CATCH observatory in Mali (Mougin et al., 2009), indicating the importance of hydro-climatic conditions during the so-called fast growth period which extends from the end of establishment period till flowering (Penning de Vries and Djiteye, 1982).

Generally, it is considered that rainfall governs the inter-annual variation in vegetation productivity for the Sahel (e.g. Fensholt et al., 2013; Hickler et al., 2005). The lack of relationship between spatial and inter-annual dynamics in GPP and rainfall (Table 5, Fig. 5) could possibly be explained by human impact degrading the rain use efficiency (GPP/rainfall) since the Wankama sites had the lowest ratio of GPP to rainfall (Fig. 5). The Wankama plots are typical of the conditions prevailing over the whole Fakara region of SW Niger, an area with a strong reduction in vegetation productivity which has mainly been attributed to a strong human impact due to land use intensification, a strong grazing pressure, wood harvesting, soil loss, and decreased fertility (Cappelaere et al., 2009; Dardel et al., 2014). As is observed in the Wankama fields, increasing cropping and grazing intensity and shortening of fallow duration on poor soils with very little fertilizing and anti-erosion measures, can explain this depressed productivity, and hence the low rain use efficiency. This ratio also directly suffers from the propensity of the Fakara soils to develop surface crusting that hampers rain infiltration, a property that has been enhanced by the type of land management and is prevailing in the Wankama fields (Velluet et al., 2014). The decoupling between rainfall and GPP could also be explained by site specific conditions of run-on, run-off, percolation or as direct wet evaporation (e.g. Timouk et al., 2009; Velluet et al., 2014). Yet another explanation could be related to the available species pool in the Sahel being adapted to dry conditions (Elberse and Breman, 1990), and once the water is sufficient for growth, productivity is no longer limited by rainfall (Hiernaux et al., 2009).

On the other hand, it has also been shown that a false start of the rainy season could strongly alter the herbaceous species composition with strong effects on biomass accumulation (Mbow et al., 2013). Soil water availability is thereby an important factor for seasonal dynamics in vegetation productivity, supported by SWC being the most important hydro-climatic variable related to seasonal dynamics in GPP (Table 3). Another factor with a strong correlation to the flux processes was Rh. The most far western station, Dahra has very high fluxes in relation to other semi-arid savanna sites. This has been explained by alleviated water stress conditions,

Table 4
Annual budgets of the land atmosphere exchange processes for the different sites and the different years. NEE is net ecosystem exchange, GPP is gross primary productivity, R_{eco} is ecosystem respiration. The sites are Demokeya (SD-Dem), Agoufou (ML-AgG), Kelma (ML-Kem), Dahra (SN-Dah), Wankama Fallow (NE-WaF), and Wankama Millet (NE-WaM). The annual budgets are given ± total errors. Errors within brackets are1) errors for individual turbulent flux measurements (E_{meas}), 2) ± errors related to gap filling using light response functions (E_{gap_light}), 3) ± errors associated with the gap-filling using the average night-time data and the mean diurnal variation (E_{gap_mean}) and 4) ± errors associated with filling gaps longer than 3 days using regression tree analysis (E_{gap_tree}).

Site	Year	NEE (g C m^{-2} y^{-1})	GPP (g C m^{-2} y^{-1})	R_{eco} (g C m^{-2} y^{-1})
SD-Dem	2007	−121 ± 43 (18 ± 2 ± 4 ± 19)	433 ± 44 (22 ± 3 ± 4 ± 15)	366 ± 26 (13 ± 1 ± 5 ± 7)
SD-Dem	2008	−131 ± 44 (20 ± 15±4 ± 5)	520 ± 80 (57 ± 16 ± 3 ± 4)	408 ± 49 (38 ± 5 ± 4 ± 2)
SD-Dem	2009	−87 ± 25 (13 ± 4 ± 4 ± 4)	461 ± 73 (55 ± 4 ± 8 ± 6)	383 ± 48 (41 ± 2 ± 4 ± 1)
ML-AgG	2007	−89 ± 31 (14 ± 1 ± 4 ± 12)	414 ± 54 (37 ± 1 ± 7 ± 9)	332 ± 31 (23 ± 1 ± 3 ± 4)
ML-Kem	2007	−309 ± 106(73 ± 8 ± 15 ± 10)	1058 ± 160 (132 ± 17 ± 2 ± 9)	744 ± 112(66 ± 4 ± 11 ± 31)
SN-Dah	2010	−373 ± 80 (28 ± 6 ± 15 ± 31)	1301 ± 124(65 ± 14 ± 10 ± 35)	937 ± 94 (37 ± 9 ± 14 ± 34)
SN-Dah	2011	−230 ± 51 (29 ± 4 ± 7 ± 11)	959 ± 112 (89 ± 5 ± 1 ± 17)	788 ± 92 (60 ± 5 ± 6 ± 21)
SN-Dah	2012	−221 ± 40 (15 ± 9 ± 12 ± 4)	1030 ± 116 (79 ± 17 ± 12 ± 8)	829 ± 77 (61 ± 3 ± 9 ± 4)
SN-Dah	2013	−225 ± 66 (15 ± 9 ± 24 ± 18)	881 ± 134 (51 ± 67 ± 2 ± 14)	609 ± 63 (35 ± 3 ± 12 ± 13)
NE-WaF	2005	−137 ± 37 (5 ± 13 ± 8 ± 11)	495 ± 63 (29 ± 17 ± 7 ± 10)	397 ± 40 (24 ± 2 ± 8 ± 6)
NE-WaF	2006	−107 ± 26 (9 ± 9 ± 8 ± 0)	568 ± 78 (61 ± 13 ± 2 ± 2)	474 ± 59 (49 ± 1 ± 8 ± 1)
NE-WaM	2005	−63 ± 34 (8 ± 3 ± 13 ± 10)	461 ± 54 (40 ± 4 ± 4 ± 6)	428 ± 45 (31 ± 4 ± 9 ± 1)
NE-WaM	2006	−10 ± 29 (7 ± 3 ± 17 ± 2)	414 ± 58 (42 ± 11 ± 2 ± 3)	403 ± 40 (31 ± 5 ± 4 ± 0)
Average		−162 ± 48 (20 ± 7 ± 10 ± 11)	692 ± 89 (58 ± 15 ± 5 ± 11)	546 ± 59 (39 ± 3 ± 7 ± 10)

Table 5
Correlation matrix between spatial and inter-annual variability in CO_2 flux processes and the explanatory variables. NEE is net ecosystem exchange; GPP is gross primary productivity; R_{eco} is ecosystem respiration; P is annual rainfall; T_{air} and T_{soil} are yearly averaged air temperature at 2 m height and soil temperature at 0.1 m depth, respectively; SWC is yearly averaged soil water content (% volumetric water content) measured at 0.1 m depth; Rh is yearly averaged relative humidity; VPD is yearly averaged vapour pressure deficit; R_g is yearly averaged incoming global radiation; N and C cont. are soil nitrogen and carbon contents; G.S. is growing season; LAI_{max} is maximum leaf area index; $FPAR_{max}$ is maximum fraction of photosynthetically active radiation absorbed by the vegetation; $NDVI_{max}$ is maximum normalized difference vegetation index (NDVI); $NDVI_{sum}$ is annual sum of NDVI; and $NDVI_{int}$ is growing season integral of NDVI. Sample size was 13 for all except the marked explanatory variables.

Explanatory variable	NEE($g C m^{-2} y^{-1}$)	GPP($g C m^{-2} y^{-1}$)	R_{eco}($g C m^{-2} y^{-1}$)
Meteorological data			
P (mm)	−0.21	0.39	0.49*
T_{air} (°C)	0.09	−0.06	−0.07
T_{soil} (°C)[a]	−0.44	0.45	0.46
SWC (%)[b]	−0.50	0.53	0.52
Rh (%)	−0.61*	0.72**	0.75**
VPD (hPa)	−0.08	0.16	0.20
R_g ($W m^{-2}$)	0.39	−0.58*	−0.63*
Biomass and edaphic data			
Biomass($g DW m^{-2}$)[b]	−0.75**	0.82**	0.80**
C3/C4 ratio	−0.17	0.02	−0.05
N cont. (%)[c]	−0.63	0.57	0.50
C cont. (%)[c]	−0.82**	0.88**	0.86**
Earth observation data			
G.S. start	0.31	−0.31	−0.32
G.S. end	0.44	−0.46	−0.44
G.S. length	0.28	−0.34	−0.33
LAI_{max}	−0.94**	0.94**	0.90**
$FPAR_{max}$	−0.92**	0.93**	0.90**
$NDVI_{max}$	−0.93**	0.94**	0.89**
$NDVI_{sum}$	−0.87**	0.87**	0.83**
$NDVI_{int}$	−0.94**	0.95**	0.90**
Flux data[d]			
NEE		−0.95**	−0.89**
GPP			0.98**
R_{eco}			

[a] Sample size equals 12.
[b] Sample size equals 11.
[c] Sample size equals 9.
[d] Spurious correlation taken into account (see main text Section 2.3.3).
* Significant at 0.05 level.
** Significant at 0.01 level.

a low C3/C4 ratio and a grazing pressure resulting in compensatory growth and fertilization effects (Tagesson et al., 2016). Yet another reason could be the West African Monsoon with reversed winds during the warmer part of the year. During the rainy season, south-western winds bring a humid layer of surface air from the Atlantic, possibly increasing vegetation productivity for the most western part of Sahel.

Phenology of the vegetation, derived from earth observation data, was the main explanatory variable coupled to seasonal, inter-annual and spatial dynamics in all CO_2 fluxes (Table 5). By applying the empirical relationship in Fig. 4a on $NDVI_{int}$ estimates across the Sahel, a rough and indicative regional-scale NEE can be calculated. Average NEE 2005–2013 would be $-149 g C m^{-2} y^{-1}$, and with a size of 3 million km^2 this equals a mean NEE uptake of $-448 Tg C y^{-1}$ for the entire region. This is a substantial fraction (~4.5%) of the global C emissions from fossil fuel and land-use change, $\sim 10 Pg C y^{-1}$, and hereby a significant contributor to the important CO_2 uptake by terrestrial ecosystems (Ahlström et al., 2015; Le Quéré et al., 2013). A strong greening trend in the Sahel has been observed from satellite observations during the last three decades due to alleviated water stress conditions (e.g. Dardel et al., 2014; Fensholt et al., 2013; Olsson et al., 2005), possibly indicating that a substantial part of the absorbed C increases the biomass

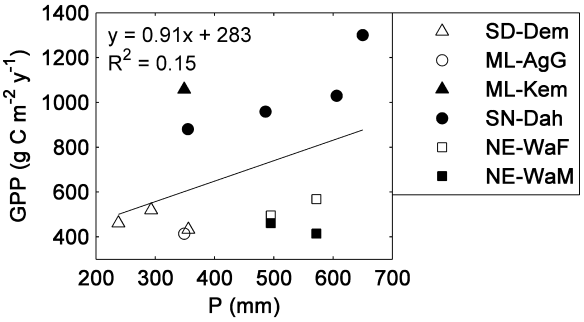

Fig. 5. Scatter plot of among-site and inter-annual budgets of gross primary productivity (GPP) against annual rainfall (P; mm y^{-1}). The different sites are Demokeya (SD-Dem), Agoufou (ML-AgG), Kelma (ML-Kem), Dahra (SN-Dah), Wankama Fallow (NE-WaF), and Wankama Millet (NE-WaM). The black line is the ordinary least-square linear regression line.

density for the Sahel. However, there was no greening trend at the Dahra field site 2002–2012 (Tagesson et al., 2015b), where instead it was shown that a main part of the absorbed C ends up in the soil organic C pool (Tagesson et al., 2016). It has also been shown that the CO_2 released by wildfires is higher than the emissions by fossil fuel burning for Africa, and 52% of the worlds total fire emissions originates from Africa (Valentini et al., 2014; Williams et al., 2007). It is hereby of urgent matter to further study, quantify and up-scale these fluxes to fully understand the land-atmosphere C exchange processes across the vast areas of Sahel.

There is considerable uncertainty in the projections of future climate for the Sahel, but an average increase in temperature for the region is expected. A decrease in rainfall for the western Sahel, and an increase in rainfall for the eastern part is also projected (Roehrig et al., 2013). This points to a continuous strong C sink for the eastern Sahel, whereas the sink of the western Sahel could decrease, and it may even turn into a source of the C accumulated during years of alleviated water stress conditions.

5. Conclusions

In this study including available NEE data for six eddy covariance flux sites across the Sahel, we have found that all sites were net sinks of atmospheric CO_2, but both NEE and its components (GPP and R_{eco}) were highly variable both in time and space. Variability in GPP was higher compared with R_{eco}, and factors regulating GPP are thereby fundamental for determining the inter-annual variability in the C balance of the Sahel. It was shown that once the water is sufficient for growth, GPP is no longer limited by rainfall. Instead, vegetation phenology, and seasonal dynamics in SWC were found to be important factors for determining GPP variability. At diurnal scale, PAR was the main driving factor determining GPP variability. Vegetation productivity was the main factor determining diurnal variability in R_{eco}, whereas seasonal variability was strongly coupled to phenology and GPP. A rough regional-scale NEE estimate indicated that the Sahel, during the period of analysis, was a significant contributor to the important land C sink. It is of thereby of major importance to study effects of climate change on vegetation properties, and seasonal dynamics in SWC, and to include these factors into models of current and future C exchange process levels for the Sahel.

Acknowledgements

Data is available from Fluxnet (http://fluxnet.ornl.gov) and CarboAfrica (http://www.carboafrica.net/index_en.asp). Data for the Mali and Niger sites were made available by the AMMA-CATCH regional observatory (www.amma-catch.org), which is primarily

funded by the French Institut de Recherche pour le Développement (IRD) and Institut National des Sciences de l'Univers (INSU). The project was funded by the Danish Council for Independent Research (DFF) Sapere Aude programme. Faculty of Science, Lund University supported the Dahra and Demokeya measurements with an infrastructure grant. Ardö received support from the Swedish National Space Board. Finally, the anonymous reviewers are thanked for detailed and constructive comments.

References

Abdi, A., Seaquist, J., Tenenbaum, D., Eklundh, L., Ardö, J., 2014. The supply and demand of net primary production in the Sahel. Environ. Res. Lett. 9, 094003.
Ahlström, A., et al., 2015. The dominant role of semi-arid ecosystems in the trend and variability of the land CO_2 sink. Science 348 (6237), 895–899.
Ardö, J., Mölder, M., El-Tahir, B., Elkhidir, H., 2008. Seasonal variation of carbon fluxes in a sparse savanna in semi arid Sudan. Carbon Balance Manag. 3 (1), 7.
Aubinet, M., et al., 2001. Long term carbon dioxide exchange above a mixed forest in the Belgian Ardennes. Agric. For. Meteorol. 108 (4), 293–315.
Bai, Z.G., Dent, D.L., Olsson, L., Schaepman, M.E., 2008. Proxy global assessment of land degradation. Soil Use Manag. 24 (3), 223–234.
Baldocchi, D., et al., 2001. FLUXNET: a new tool to study the temporal and spatial variability of ecosystem–scale carbon dioxide, water vapor, and energy flux densities. Bull. Am. Meteorol. Soc. 82 (11), 2415–2434.
Boulain, N., et al., 2009. Towards an understanding of coupled physical and biological processes in the cultivated Sahel—2. Vegetation and carbon dynamics. J. Hydrol. 375 (1–2), 190–203.
Brümmer, C., et al., 2008. Diurnal, seasonal, and interannual variation in carbon dioxide and energy exchange in shrub savanna in Burkina Faso (West Africa). J. Geophys. Res. 113 (G2), G02030.
Brett, M.T., 2004. When is a correlation between non-independent variables spurious? Oikos 105 (3), 647–656.
Cappelaere, B., et al., 2009. The AMMA-CATCH experiment in the cultivated Sahelian area of south-west Niger—Investigating water cycle response to a fluctuating climate and changing environment. J. Hydrol. 375 (1–2), 34–51.
Dardel, C., et al., 2014. Re-greening Sahel: 30 years of remote sensing data and field observations (Mali, Niger). Remote Sens. Environ. 140, 350–364.
De'ath, G., Fabricius, K.E., 2000. Classification and regression trees: a powerful yet simple technique for ecological data analysis. Ecology 81 (11), 3178–3192.
Elberse, W.T., Breman, H., 1989. Germination and establishment of Sahelian rangeland species: I. Seed properties. Oecologia 80, 477–484.
Elberse, W.T., Breman, H., 1990. Germination and establishment of Sahelian rangeland species II. Effects of water availability. Oecologia 85, 32–40.
Falge, E., et al., 2001. Gap filling strategies for defensible annual sums of net ecosystem exchange. Agric. For. Meteorol. 107 (1), 43–69.
Fensholt, R., et al., 2013. Assessing land degradation/recovery in the African Sahel from long-term earth observation based primary productivity and precipitation relationships. Remote Sens. 5, 664–686.
Fensholt, R., et al., 2015. Global-scale mapping of changes in ecosystem functioning from earth observation-based trends in total and recurrent vegetation. Global Ecol. Biogeogr. 24 (9), 1003–1017.
Flanagan, L.B., Johnson, B.G., 2005. Interacting effects of temperature, soil moisture and plant biomass production on ecosystem respiration in a northern temperate grassland. Agric. For. Meteorol. 130 (3–4), 237–253.
Hickler, T., et al., 2005. Precipitation controls Sahel greening trend. Geophys. Res. Lett. 32, L21415.
Hiernaux, P., et al., 2009. Rangeland response to rainfall and grazing pressure over two decades: herbaceous growth pattern production and species composition in the Gourma. Mali. J. Hydrol. 375 (1–2), 114–127.
Jönsson, P., Eklundh, L., 2004. TIMESAT—a program for analyzing time-series of satellite sensor data. Comput. Geosc. 30 (8), 833–845.
Janssens, I.A., et al., 2001. Productivity overshadows temperature in determining soil and ecosystem respiration across European forests. Global Change Biol. 7 (3), 269–278.
Lasslop, G., Reichstein, M., Papale, D., 2010. Separation of net ecosystem exchange into assimilation and respiration using a light response curve approach: critical issues and global evaluation. Global Change Biol. 16 (1), 187–208.
Le Quéré, C., et al., 2013. The global carbon budget 1959–2011. Earth Syst. Sci. Data 5 (1), 165–185.
Lindroth, A., Klemedtsson, L., Grelle, A., Weslien, P., Langvall, O., 2008. Measurement of net ecosystem exchange, productivity and respiration in three spruce forests in Sweden shows unexpectedly large soil carbon losses. Biogeochemistry 89 (1), 43–60.
Lloyd, J., Taylor, J.A., 1994. On the temperature dependence of soil respiration. Funct. Ecol. 8 (3), 315–323.
Lund, M., et al., 2010. Variability in exchange of CO_2 across 12 northern peatland and tundra sites. Global Change Biol. 16 (9), 2436–2448.
Mayaux, P., et al., 2003. EUR 20665 EN—A Land-cover Map of Africa. European Commisions Joint Research Centre, Luxembourg (38 pp).
Mbow, C., Fensholt, R., Rasmussen, K., Diop, D., 2013. Can vegetation productivity be derived from greenness in a semi-arid environment? Evidence from ground-based measurements. J. Arid Environ. 97, 56–65.
Merbold, L., et al., 2009. Precipitation as driver of carbon fluxes in 11 African ecosystems. Biogeosciences 6 (6), 1027–1041.
Moncrieff, J.B., Malhi, Y., Leuning, R., 1996. The propagation of errors in long-term measurements of land-atmosphere fluxes of carbon and water. Global Change Biol. 2 (3), 231–240.
Moncrieff, J.B., et al., 1997. Spatial and temporal variations in net carbon flux during HAPEX-Sahel. J. Hydrol. 188–189 (1–4), 563–588.
Mougin, E., et al., 2009. The AMMA-CATCH Gourma observatory site in Mali: relating climatic variations to changes in vegetation, surface hydrology, fluxes and natural resources. J. Hydrol. 375 (1–2), 14–33.
OECD, 2009. Chapter 15. Vulnerability in the sahelian zone. In: Bossard, L. (Ed.), West African Studies: Regional Atlas on West Africa. OECD Publishing, Paris, pp. 269–284.
Olsson, L., Eklundh, L., Ardö, J., 2005. A recent greening of the Sahel—trends, patterns and potential causes. J. Arid Environ. 63 (3), 556–566.
Papale, D., et al., 2006. Towards a standardized processing of Net Ecosystem Exchange measured with eddy covariance technique: algorithms and uncertainty estimation. Biogeosciences 3 (4), 571–583.
Papale, D., 2012. Data gap filling. In: Aubinet, M., Vesala, T., Papale, D. (Eds.), Eddy Covariance— A Practical Guide to Measurement and Data Analysis. Springer, Dordrecht, pp. 159–172.
Penning deVries, F.W.T., Djiteye, M.A., 1982. La productivité des pâturages sahéliens, une étude des sols, des végétations et de l'exploitation de cette ressource naturelle. Pudoc Wageningen (525 pp).
Poulter, B., et al., 2014. Contribution of semi-arid ecosystems to interannual variability of the global carbon cycle. Nature 509 (7502), 600–603.
Prince, S.D., et al., 1995. Geographical, biological and remote sensing aspects of the hydrologic atmospheric pilot experiment in the sahel (HAPEX-Sahel). Remote Sens. Environ. 51 (1), 215–234.
Ramier, D., et al., 2009. Towards an understanding of coupled physical and biological processes in the cultivated Sahel–1. Energy and water. J. Hydrol. 375 (1–2), 204–216.
Reichstein, M., Stoy, P.C., Desai, A.R., Lasslop, G., Richardson, A.D., 2012. Chapter 9. partitioning of net fluxes. In: Aubinet, M., Vesala, T., Papale, D. (Eds.), Eddy Covariance—A Practical Guide to Measurement and Data Analysis. Springer, Dordrecht, pp. 263–290.
Reichstein, M., et al., 2005. On the separation of net ecosystem exchange into assimilation and ecosystem respiration: review and improved algorithm. Global Change Biol. 11 (9), 1424–1439.
Richter, K., Atzberger, C., Hank, T.B., Mauser, W., 2012. Derivation of biophysical variables from Earth observation data: validation and statistical measures. J. Appl. Remote Sens. 6 (1), 063557.
Rockström, J., de Rouw, A., 1997. Water, nutrients and slope position in on-farm pearl millet cultivation in the Sahel. Plant Soil 195 (2), 311–327.
Roehrig, R., Bouniol, D., Guichard, F., Hourdin, F., Redelsperger, J.L., 2013. The present and future of the west african monsoon: a process-Oriented assessment of CMIP5 simulations along the AMMA transect. J. Clim. 26 (17), 6471–6505.
Sarr, B., 2012. Present and future climate change in the semi-arid region of West Africa: a crucial input for practical adaptation in agriculture. Atmos. Sci. Lett. 13 (2), 108–112.
Schwalm, C.R., et al., 2010. Assimilation exceeds respiration sensitivity to drought: a FLUXNET synthesis. Global Change Biol. 16 (2), 657–670.
Sjöström, M., et al., 2009. Evaluation of satellite based indices for gross primary production estimates in a sparse savanna in the Sudan. Biogeosciences 6 (1), 129–138.
Tagesson, T., et al., 2015a. Dynamics in carbon exchange fluxes for a grazed semi-arid savanna ecosystem in West Africa. Agric. Ecosyst. Environ. 205, 15–24.
Tagesson, T., et al., 2015b. Ecosystem properties of semi-arid savanna grassland in West Africa and its relationship to environmental variability. Global Change Biol. 21 (1), 250–264.
Tagesson, T., et al., 2016. Very high carbon exchange fluxes for a grazed semi-arid savanna ecosystem in West Africa. Danish J. Geogr. (accepted).
Tang, J., Baldocchi, D.D., Xu, L., 2005. Tree photosynthesis modulates soil respiration on a diurnal time scale. Global Change Biol. 11 (8), 1298–1304.
Timouk, F., et al., 2009. Response of surface energy balance to water regime and vegetation development in a Sahelian landscape. J. Hydrol. 375 (1-2), 178-189.
Tucker, C.J., Vanpraet, C., Boerwinkel, E., Gaston, A., 1983. Satellite remote sensing of total dry matter production in the Senegalese Sahel. Remote Sens. Environ. 13 (6), 461–474.
Valentini, R., et al., 2014. A full greenhouse gases budget of Africa: synthesis, uncertainties, and vulnerabilities. Biogeosciences 11 (2), 381–407.
Velluet, C., et al., 2014. Building a field- and model-based climatology of local water and energy cycles in the cultivated Sahel; annual budgets and seasonality. Hydrol. Earth Syst. Sci. 18 (12), 5001–5024.
Williams, C., et al., 2007. Africa and the global carbon cycle. Carbon Balance Manag. 2 (1), 3.